Benchmarking Perturbation-based Saliency Maps for Explaining Deep Reinforcement Learning Agents

Tobias Huber, 1* Benedikt Limmer, 1* Elisabeth André 1

¹ University of Augsburg, Augsburg, Germany tobias.huber@uni-a.de, benedikt.limmer@student.uni-augsburg.de, andre@informatik.uni-augsburg.de

Abstract

Recent years saw a plethora of work on explaining complex intelligent agents. One example is the development of several algorithms that generate saliency maps which show how much each pixel attributed to the agents' decision. However, most evaluations of such saliency maps focus on image classification tasks. As far as we know, there is no work which thoroughly compares different saliency maps for Deep Reinforcement Learning agents. This paper compares four perturbation-based approaches to create saliency maps for Deep Reinforcement Learning agents trained on four different Atari 2600 games. All four approaches work by perturbing parts of the input and measuring how much this affects the agent's output. The approaches are compared using three computational metrics: dependence on the learned parameters of the agent (sanity checks), faithfulness to the agent's reasoning (input degradation) and run-time.

1 Introduction

With the rapid development of machine learning methods, Intelligent Agents powered by Deep Reinforcement Learning (DRL), are making their way into increasingly high risk applications, such as healthcare and robotics (Stone et al. 2016). However, with the growing complexity of these algorithms, it is hardly if at all possible to comprehend the decisions of the resulting agents (Selbst and Barocas 2018). The research areas of Explainable Artificial Intelligence (XAI) and Interpretable Machine Learning aim to shed light on the decision-making process of existing black-box models. In the case of Neural Networks with visual inputs, the most common explanation approach is the generation of saliency maps that highlight the most relevant input pixels for a given prediction. Recent years saw a plethora of methods to create such saliency maps (Arrieta et al. 2020). However, a current challenge for XAI is finding suitable measures for evaluating these explanations. For black-box models like deep neural networks, it is especially crucial to evaluate the faithfulness of the explanations (i.e., is the reasoning given by the explanation the same reasoning which the agent actually used) (Mohseni, Zarei, and Ragan 2020). This need for evaluating the faithfulness of explanations was further demonstrated by

Adebayo et al. (2018), who proposed sanity checks which showed that for some saliency approaches, there is no strong dependence between the agents learned parameters and the resulting saliency maps.

So far, most faithfulness comparisons of saliency maps focus on image classification tasks. There is little work on computationally evaluating saliency maps in different tasks like Reinforcement Learning. Furthermore, these evaluations often try to cover as many different saliency map approaches as possible. This mostly leads to selections of algorithms with distinct motivations and requirements, which is less helpful for people with specific requirements. Without full access to the agent, for example, one cannot use methods that rely on the inner workings of the agent but must rely on model agnostic methods, which can be applied to any agent. Model agnostic saliency maps mostly come in the form of perturbation-based approaches which perturb parts of the input and observe how much this affects the agent's prediction.

This work presents a computational comparison of four perturbation-based saliency map approaches: the original Occlusion Sensitivity approach (Zeiler and Fergus 2014), Local Interpretable Model-agnostic Explanations (LIME) (Ribeiro, Singh, and Guestrin 2016), a *Noise Sensitivity* approach proposed for DRL (Greydanus et al. 2018), and Randomized Input Sampling for Explanation (RISE) (Petsiuk, Das, and Saenko 2018). As the main task, we use a DRL Agent trained on four Atari 2600 games, and an emotion recognition task as secondary applications to test the approaches model agnosticism. As metrics, we use the sanity checks proposed by Adebayo et al. (2018), an insertion metric which slowly inserts the most important pixels of the input and a run-time analysis. As far as we know, this is the first time that sanity checks were done for perturbationbased saliency maps and the first direct comparison of how faithful different perturbation-based saliency maps are.

2 Related Work

The XAI literature is rapidly growing in recent years. In this work, we focus on saliency maps that highlight the areas of the input which were important for the agents' decision. There are three main ideas on how to create saliency maps. The first idea is to use the gradient with respect to each input to see how much small changes of this input influence the

^{*}These authors contributed equally to this work. Copyright © 2021, Association for the Advancement of Artificial Intelligence (www.aaai.org). All rights reserved.

prediction (Simonyan, Vedaldi, and Zisserman 2014; Sundararajan, Taly, and Yan 2017; Selvaraju et al. 2020). These approaches require the underlying agent to be differentiable. Other methods use modified propagation rules to calculate how relevant each neuron of the network was, based on the intermediate results of the prediction. Examples for this are Layer-wise Relevance Propagation (LRP) (Bach et al. 2015) or PatternAttribution (Kindermans et al. 2018). This idea requires access to the inner-workings of the agent. Finally, perturbation-based approaches perturb areas of the input and measure how much this changes the output of the agent. The major advantage of perturbation-based approaches over the aforementioned methods is their model agnosticism. Since they only use the in- and outputs of the agent, they can be applied to any agent without adjustments.

The evaluation metrics for XAI approaches can be separated into two broad categories: human user-studies and computational measurements (Mohseni, Zarei, and Ragan 2020). Examples of human user-studies of saliency maps for DRL agents are (Huber et al. 2020) and (Anderson et al. 2019), who evaluate LRP and Noise Sensitivity saliency maps respectively, with regards to mental models, trust and user satisfaction. To obtain more objective quantitative data it is important to additionally evaluate explanations through computational measurements. Such measurements also provide an easy way to collect preliminary data before recruiting users for a user study.

The most common computational measurement for saliency maps is input degradation. Here, the input of the agent is gradually deleted, starting with the most relevant input features according to the saliency map. In each step, the agent's confidence is measured. If the saliency maps faithfully describe the agent's reasoning, then the agent's confidence should fall quickly. For visual input this is either done by deleting a single pixel per step (Petsiuk, Das, and Saenko 2018; Ancona et al. 2018) or by deleting patches of the image in each step (Samek et al. 2017; Kindermans et al. 2018; Schulz et al. 2020). In addition to deleting features, some newer approaches also propose a insertion metric where they start with "empty" inputs and gradually insert input features (Ancona et al. 2018; Petsiuk, Das, and Saenko 2018; Schulz et al. 2020). The aforementioned image degradation tests mostly compared several gradient-based methods and one or two perturbation-based and modified propagation approaches. As of now, there are no direct comparisons of different perturbation-based saliency maps. Furthermore, all previous tests use image classification tasks for their degradation measurements. As far as we know, there are no input degradation benchmarks for Reinforcement Learning tasks.

Another computational measurement for saliency maps are the so called *sanity checks* proposed by Adebayo et al. (2018). These tests measure whether the saliency map is dependent on what the agent learned. One method for this is gradually randomizing the layers of the neural network and measuring how much this changes the saliency maps. Adebayo et al. did this for various gradient-based approaches and Sixt, Granz, and Landgraf (2019) additionally tested LRP methods. As far as we know, there is no work that computed sanity checks for perturbation-based saliency maps

even though this is one of the most popular saliency maps approaches.

3 Experiments

This section presents the test-beds used in this work, the four perturbation-based saliency map approaches which were compared, and the metrics used to evaluate the approaches. The code for all experiments is available online¹.

The main test-bed in our paper is the Atari Learning Environment (Bellemare et al. 2013). Four DRL agents were trained on the games MsPacman (Simplified to Pac-Man in this work), Space Invaders, Frostbite, and Breakout using the Deep Q-Network (DQN) (Mnih et al. 2015) implementation of the OpenAI Baselines Framework (Dhariwal et al. 2017). The agents make predictions by observing the last 4 frames of the game and then choose from a pool of possible actions. Hereby, each frame is down-sampled and greyscaled resulting in $84\times84\times4$ input images. To normalize the output values between different inputs, we use a softmax activation function to obtain an actual probability for each action.

One advantage of perturbation-based saliency maps is that they don't depend on specific kinds of agents. To properly evaluate how the algorithms perform on different agents, we additionally tested them on an emotion recognition network, which uses the VGG-Face architecture (Parkhi, Vedaldi, and Zisserman 2015) to differentiate between 8 emotions on images of human faces. The network was trained on the AffectNet dataset consisting of RGB images of variable size (Mollahosseini, Hasani, and Mahoor 2017).

The basic saliency map generation process is the same between all four approaches compared in this work. Let f be the agent that takes a visual input I and maps it to a confidence value for each possible action or emotion. Without loss of generality, f(I) describes the confidence in the agent's original prediction. That is, the action or emotion which the agent chooses for the unperturbed image. An input image I with height H and width W can be defined as a mapping $I:\Lambda_I\to\mathbb{R}^c$ of each pixel $\lambda\in\Lambda_I=\{1,...,H\}\times\{1,...,W\}$ to c channels (e.g. c=4 for the Atari environment). To determine the relevance of each pixel λ for the prediction of the agent, all four approaches feed perturbed versions of I to the agent and then compare the resulting confidence values with the original results. However, the approaches widely differ in the way the image is perturbed and how the relevance per pixel is computed:

Occlusion Sensitivity (Zeiler and Fergus 2014): This approach creates perturbed images I' by shifting a grey 5×5 (20×20 for Affectnet) patch across the original image I (i.e. setting the values of the pixels inside this patch to half of the maximum color value). The importance $S(\lambda)$ of each pixel λ inside the patch is then computed based on the agents' confidence after the perturbation

$$S(\lambda) = 1 - f(I'). \tag{1}$$

Since the original source does not go into details about the algorithm, we use the *tf-explain* implementation as reference (tf explain 2019).

¹https://github.com/belimmer/PerturbationSaliencyEvaluation

Noise Sensitivity (Greydanus et al. 2018): Instead of completely occluding patches of the image, this approach adds noise to the image I by applying a Gaussian blur to a circle with radius r (in our case r=5) around a pixel λ . The modified image $I'(\lambda)$ is then used to compute the importance of the covered circle, by comparing the agent's logit units $\pi(x)$ (i.e. the outputs of all output neurons before softmax):

$$S(\lambda) = \frac{1}{2} ||\pi(I) - \pi(I'(\lambda))||^2$$
 (2)

This is done for every 5th pixel resulting in a temporary saliency map which is smaller than the input. For the final saliency map, the result is up-sampled using bilinear interpolation.

RISE (Petsiuk, Das, and Saenko 2018): This approach uses a set of N=2000 randomly generated masks $\{M_1,...,M_N\}$ for perturbation. To this end, temporary 8×8 masks are created by setting each element to 1 with a probability p=0.9 (p=0.4 for Affectnet) and 0 otherwise. These temporary masks are upsampled to the size of the input image using bilinear interpolation. The images are perturbed by element-wise multiplication with those masks $I\odot M_i$. The relevance of each pixel λ is given by

$$S(\lambda_I) = \frac{1}{p \cdot N} \sum_{i=1}^{N} f(I \odot M_i) \cdot M_i(\lambda), \tag{3}$$

where $M_i(\lambda)$ denotes the value of the pixel λ in the ith mask. LIME (Ribeiro, Singh, and Guestrin 2016): The original image is divided into superpixels using segmentation algorithms (we use the default Quickshift algorithm with slightly adjusted parameters). Perturbed variations of the image are generated by "deleting" different combinations of superpixels (i.e. setting all pixels of the superpixels to 0). The combination of occluded images and the corresponding predictions by the agent are then used to train a locally weighted interpretable model for 1000 steps. Analyzing the weights of this local model provides a relevance value for each superpixel.

The saliency maps of the four different approaches are evaluated with three different computational metrics:

Sanity Checks: The parameter randomization test proposed by Adebayo et al. (2018) measures the dependence between the saliency maps and the parameters learned by the neural network of the agent. To this end, the parameters of each layer in the network are cascadingly randomized, starting with the output layer. Every time a new layer is randomized, a saliency map for this version of the agent is created. The resulting saliency maps are then compared to the saliency map for the original network, using three different similarity metrics (Spearman rank correlation, Structural Similarity (SSIM) and Pearson correlation of the histogram of gradients). If there is a strong parameter dependence then the saliency maps for the randomized model should vastly differ from the ones of the original model.

Insertion Metric: To test the premise that the most relevant pixels, according to the saliency maps, have the highest impact on the agent, the insertion metric proposed by Petsiuk, Das, and Saenko (2018) is used. We do not use a deletion metric, since we feel that it is too similar to the way that









Figure 1: Examples of perturbed input images. From left to right: Occlusion Sensitivity, Noise Sensitivity, RISE, LIME

perturbation-based saliency maps are created. The insertion metric starts with a fully occluded image (i.e. the values of all pixels are set to 0). In each step, 84 (672 for Affectnet) occluded pixels (approx. 1.2% of the full image) are uncovered, starting with the most relevant pixels according to the saliency map. For LIME, the superpixels are sorted by their relevance but the order of pixels within superpixels is randomized. The partly uncovered image is then fed to the agent and its confidence in the original prediction, which the agent chooses for the full image, is stored. If the saliency map correctly highlights the most important pixels, the models confidence should increase quickly for each partly uncovered image.

Runtime Analysis: The runtime of an algorithm can be an important aspect when choosing between different approaches. Therefore, the mean time it took each algorithm to create a single saliency map was computed using the timeit python library. To this end, saliency maps for a total of 1000 frames of the Pac-Man environment and 250 random facial expression images from the validation set of the Affectnet corpus.

4 Adjustments

Visually assessing the saliency maps for Pac-Man showed that the results produced by the original Occlusion Sensitivity (using grey patches) and the original Noise Sensitivity (using Gaussian blur) considerably vary from the ones of RISE and LIME (Fig. 2). They also did not show any consistent patterns. Similar results for Pac-Man were observed by Greydanus et al. (2018). After visualizing occluded versions of the input frame (Fig. 1) a potential problem became apparent. Both RISE and LIME use black shapes when perturbing the images, whereas Noise Sensitivity and Occlusion Sensitivity utilize grey shapes. This potentially causes the problem that the perturbation is not drastic enough and the inserted shapes are recognized as in-game objects like walls and therefore do not influence the output enough.

For Occlusion Sensitivity, this is simply fixed by changing the color from grey to black. The Noise Sensitivity approach however uses a Gaussian blur to perturb the image. Since the input frames are converted to greyscale images and the walls of the Pac-Man playing field are grey, the Gaussian blur is also predominantly grey. Because there seems to be no straight forward way to keep the blurring strategy and fix the problems, it was abandoned in favor of straight up covering the blurred region with a black circle. After these adjustments, the Occlusion Sensitivity and Noise Sensitivity mainly differ in how they calculate the importance of each

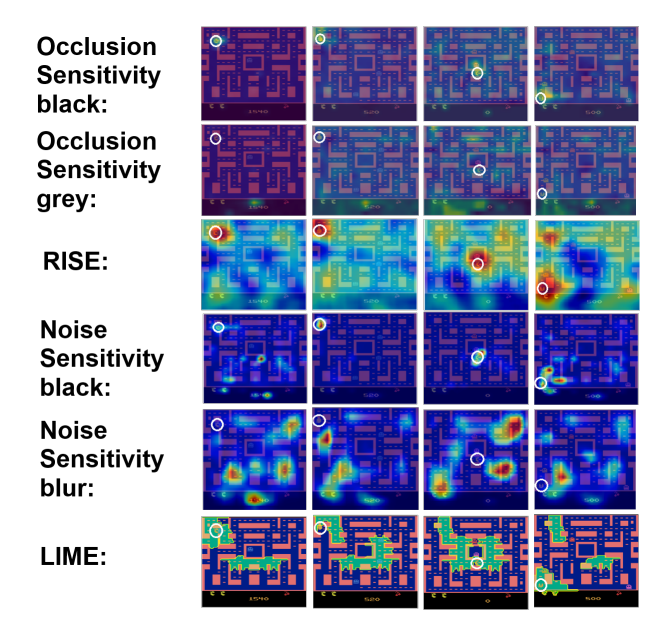


Figure 2: Example saliency maps for four different Pac-Man game states generated by each of the approaches investigated in this paper. The circles mark Pac-Man's position.

pixel (see Equations 1 and 2).

These adjustments were not necessary for the emotion recognition model. A possible explanation for this are the different domains of the models. While the Pac-Man agent uses greyscale images with a lot of grey areas, the emotion recognition model uses RGB images. Grey areas seldom occur naturally in RGB images, which makes grey patches more suited to occlude information in this domain.

5 Results

Visual Assessment: Saliency maps for the Pac-Man agent produced by all four approaches can be seen in Fig. 2. To prevent cherry picking, the Pac-Man states were chosen by the HIGHLIGHTS algorithm which was developed to select informative states about the agent's strategy (Amir and Amir 2018). The saliency maps generally seem to highlight Pac-Man and his surroundings. The saliency maps for the emotion recognition model can be seen in Fig. 3. For legal reasons we selected images that are available under the Creative Commons license.

Sanity Checks: The results of the parameter randomization test are shown in Fig. 4. They measure how similar a saliency map created for the trained agent is to saliency maps created for a cascadingly randomized agent. The lower the scores the higher the dependence on the learned parameters. It is noticeable that the SSIM score is very high across most approaches, this is because SSIM makes pixel-wise comparisons between the saliency maps. If there are only a few highlighted areas on both maps then all pixels with very small relevance values (which are barely visible in the heat maps) contribute strongly to the SSIM. The results of the other metrics are low for all approaches. Only LIME and Noise Sensitivity show less dependence on the output layer.

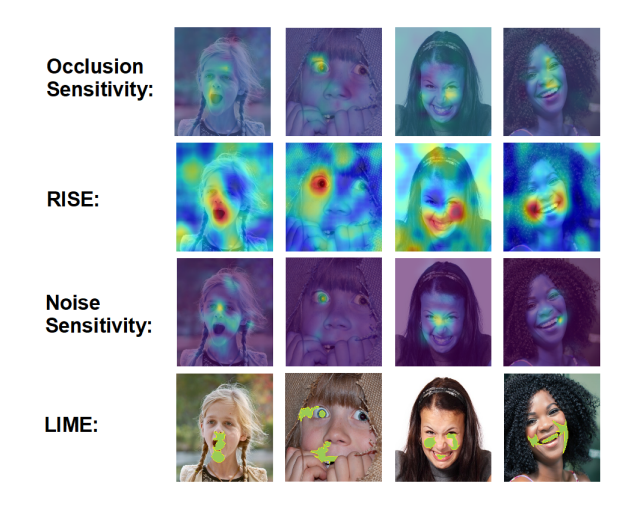


Figure 3: Example saliency maps for four different facial expressions. The emotions from left to right are: surprise, fear, disgust, and happiness. The third image was incorrectly classified as happy.

Insertion Metric: The Insertion metric measures whether the highlighted pixels actually have a high impact on the decision of the agent. The plotted results for the Atari environment can be seen in Fig. 5 and the average Area Under the Curve (AUC) values are reported in Table 1. To investigate our adjustments (section 4) we measured Occlusion Sensitivity with black and grey occlusion and Noise Sensitivity with the original Gaussian blur and with our black occlusion variant. Across all Atari games, Occlusion Sensitivity achieves the highest AUC followed by RISE. LIME and Noise Sensitivity are less clear. For the Atari environments the confidence often increases over the confidence for the full image. This is related to the fact that the agents are not perfectly sure about their actions (average confidence around 0.3). Furthermore, we use a softmax activation function which increases the confidence in the observed action when the agents confidence in other actions decreases. For the Affectnet model, LIME performs the best followed by Occlusion Sensitivity and RISE. Occlusion Sensitivity has the lowest average AUC here.

Run-time Analysis: The average run-times for each of the tested saliency map approaches are shown in Table 2. Since Occlusion Sensitivity with black and with grey color do not differ in run-time, we only report it once. There are major runtime differences between the models. For the Atari environment, Occlusion Sensitivity and the adjusted Noise Sensitivity approach, which simply occlude image patches with black pixels, perform much faster than the approaches with more complex image perturbations. For the emotion recognition model, the main difference is that LIME considerably out speeds the original Noise Sensitivity and the RISE approach. In the Atari domain, these three approaches had similar run-times. However, these results should be taken with a grain of salt since the run-time depends on the chosen hyper-parameters (e.g., segmentation algorithms in LIME).

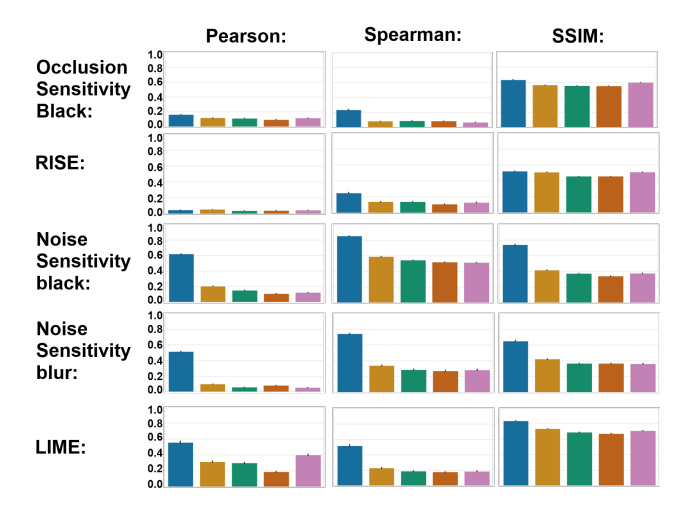


Figure 4: Results of the parameter randomization sanity check for the different perturbation-based saliency maps. Measured for 1000 steps of the Pac-Man agent. Starting from the left, each bar represents an additional randomized layer starting with the output layer (blue bar). The y-axis show the average similarity values (Pearson, Spearman, SSIM). High values indicate a low parameter dependence.

6 Discussion

Qualitative Discussion of the Saliency Maps: A visual assessment of the different saliency maps for Pac-Man (Fig. 2) shows that RISE and LIME highlight large areas of the image while Occlusion Sensitivity and Noise Sensitivity are more selective. Generally, all approaches highlight similar objects. All saliency maps focus foremost on Pac-Man itself. This is most clearly done by RISE and Occlusion Sensitivity. Noise Sensitivity sometimes highlights other areas and LIME, by its nature, highlights the whole superpixel, which includes Pac-Man, instead of focusing on Pac-Man itself. Besides that, there seems to be a focus on ghosts which are close to Pac-Man, as can be seen in the states shown in the far-left and the far-right column. Highlighting these objects makes sense from a human perspective, since the player controls Pac-Man and has to avoid regular ghosts while eating blue ghosts and pellets to gain points.

The saliency maps generated for the emotion recognition model (Fig. 3) show that RISE and LIME mostly highlight similar areas which also appear reasonable from a human point of view: the open mouth for *surprise*, an open eye for *fear*, and the mouth with raised lip corners for the two images where the model predicted *happy*. As in the Atari environment, RISE produces a lot of noise which distracts from the important areas. Occlusion Sensitivity is less clearly focused on the mouth and the raised lip corners for the happy predictions. Noise Sensitivity noticeably differs from the other approaches for the surprise and disgust images where it seems to focus on the middle of the face. This is especially interesting for the disgust image, which was misclassified as happiness by our model. This misclassification is reflected by the other approaches but not by Noise Sensitivity, which

AUC	Pac-	Space	Breakout	Frostbite	Emotion
	Man	In-			
		vaders			
OS	0.280	0.270	0.361	0.111	-
Black					
OS	0.101	0.200	0.240	0.068	0.570
Grey					
NS	0.140	0.213	0.264	0.069	-
Black					
NS	0.128	0.211	0.269	0.067	0.522
Blur					
LIME	0.156	0.206	0.291	0.067	0.714
RISE	0.207	0.229	0.304	0.073	0.623

Table 1: The average Area Under the Curve (AUC) for the graphs obtained by the insertion metric (Fig. 5). *OS* is Occlusion Sensitivity and *NS* is Noise Sensitivity. The average was computed across 1000 frames for each Atari model and 250 facial images for the Affectnet model.

Mean runtime in seconds	Pac-Man	Affectnet
Occlusion Sensitivity	0.21	18.43
Noise Sensitivity Black	0.25	-
Noise Sensitivity Blur	0.60	292.87
RISE	0.79	258.45
LIME	0.78	90.23

Table 2: The average number of seconds it took an perturbation-based approach to generate one saliency map. The average was computed across 1000 frames for the Pac-Man model and 250 facial images for the Affectnet model.

might be due to the fact that Noise Sensitivity considers all output neurons for its relevance calculation (Eq. 2).

One notable finding during the implementation of the algorithms was that adjustments to the Occlusion Sensitivity and Noise Sensitivity approach were necessary to create meaningful saliency maps for the game Pac-Man (Section 4). While occlusion with grey patches worked for the emotion recognition task, which uses RGB images as input, it did not work for the Pac-Man environment, which uses grey-scaled inputs. This shows that, while Occlusion Sensitivity and Noise Sensitivity are model agnostic, they do depend on the domain and have to be adjusted accordingly. Similarly, one has to choose a fitting segmentation algorithm for LIME and a perturbation probability p for RISE. Here, the default parameters with minor tweaks worked reasonably well for us, so we did not investigate further.

Discussion of the Sanity Checks: Fig. 4 shows the results of the parameter randomization test. When compared to the results of the sanity checks done by Adebayo et al. (2018), the perturbation-based approaches tested in our work show a strong dependence on the learned parameters of the agent. Adebayo et al. measured similarity values around 0.4 for most of the gradient-based approaches they tested. While they do measure slightly lower SSIM scores, this is mostly due to differences in the domains. The Atari Environments

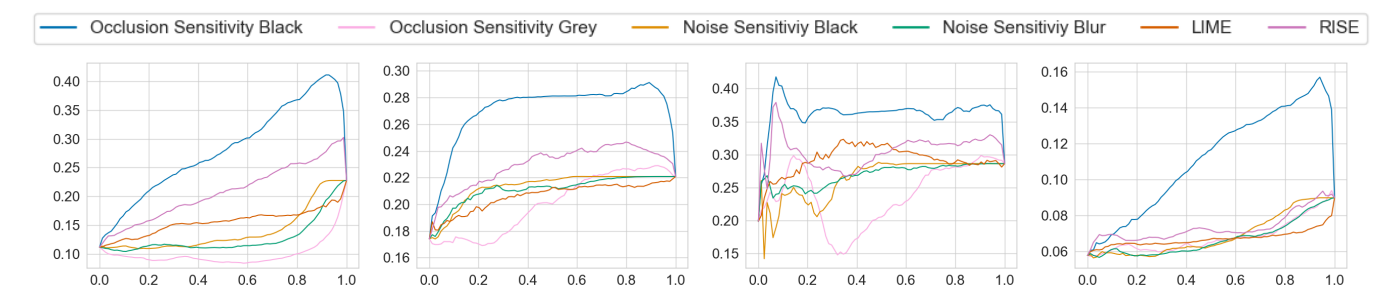


Figure 5: The insertion metric results for three different Atari games (from left to right: Pac-Man, Space Invaders, Breakout, and Frostbite), averaged over 1000 steps. The x-axis shows the percentage of inserted pixels and the y-axis shows the average confidence in the original prediction for those modified states.

used in this work contain fewer important objects which leads to more selective saliency maps with barely visible relevance values for most pixels.

When comparing the results of the different perturbationbased approaches, RISE and Occlusion Sensitivity show the highest parameter dependency. LIME demonstrates a slightly lower parameter dependence for most layers and only weak dependence on the weights of the output layer. However, this has to be taken with a grain of salt. Since LIME does not produce distinct relevance values for each pixel, the sanity check was calculated on masks where each pixel was either 1, if it was part of a highlighted superpixel, or 0 if it was not. For Noise Sensitivity, the Spearman rank correlation is higher than for the other approaches but the SSIM is lower. All similarity metrics show very weak dependence on the output layer of the agent. This might be due to the fact that Noise Sensitivity takes all actions into account instead of focusing on a single action (See Eq. 2). Another interesting observation is that replacing the Gaussian blur with black occlusion reduced the parameter dependence measured by Spearman correlation. This contrasts the fact that this adjustment led to more reasonable saliency maps and increased performance in insertion metrics for the Pac-Man agent.

Discussion of the Insertion Metric: The results of the insertion metric for the Atari environments (Fig. 5 and Table 1) are in line with the observations of the visual assessment. For all Atari environments, Occlusion Sensitivity shows the highest AUC followed by RISE, which we observed to highlight similar areas but to contain more noise. LIME takes a clear third place for Pac-Man and Breakout but performs the worse on Space Invaders and Frostbite. Across all games, Occlusion Sensitivity with grey occlusion performs the worst. Apart from the Pac-Man environment, where the original Noise Sensitivity approach was observed to generate incomprehensible saliency maps, the insertion metric does not show a strong difference between the original Noise Sensitivity approach and our adjustment that occludes black circles instead of blurring them. This shows that the main reason for the weak results of the Noise Sensitivity approach is its importance calculation (Eq. 2), which differentiates the adjusted Noise Sensitivity from Occlusion Sensitivity. A possible explanation for this is that Noise Sensitivity takes all actions into account, whereas the insertion metric only measures the confidence in a single action.

For the Affectnet model LIME places first. Occlusion Sensitivity and RISE share the second place, and Noise Sensitivity comes last. This indicates that LIME might be better suited for more complex domains like human faces, where occluding simple patches might not be enough.

7 Conclusion

This paper compared four different perturbation-based saliency map approaches measuring their dependence on the agent's parameters, their faithfulness to the agent's reasoning, and their run-time. The three most interesting findings from our experiments are:

- Occlusion Sensitivity is the best suited saliency map approach for the DRL agents tested in our experiments, followed by RISE. However, we had to change the occlusion color from grey to black to get good results. Surprisingly, Noise Sensitivity performed the worst in our tests even though it was specifically designed for this use-case. This still applies after we adjusted the algorithm to fix a potential problem in the Pac-Man game.
- When compared with previous sanity checks, all perturbation-based saliency maps tested in this paper show a high dependence on the agent's learned parameters. Only LIME and Noise Sensitivity are less dependent on the parameters of the output layer.
- Since it requires the least adjustments, RISE is suited for debugging purposes where one does not want to spend much time on fine tuning the hyper-parameters of the saliency map approach. Machine Learning practitioners should be able to discern the important information from the noisy saliency maps produced by RISE. The longer run-time of the algorithm is also not as crucial when it is not deployed in applications for end-users.

The computational measurements done in this work present a first step to fully evaluate perturbation-based saliency maps for DRL. In the future, we will build upon the insights from this paper and conduct a human user-study, similar to the one we did in (Huber et al. 2020), to evaluate how useful the saliency map approaches with good computational results are for actual end-users.

References

- Adebayo, J.; Gilmer, J.; Muelly, M.; Goodfellow, I.; Hardt, M.; and Kim, B. 2018. Sanity checks for saliency maps. In *Advances in Neural Information Processing Systems*, 9505–9515.
- Amir, D.; and Amir, O. 2018. HIGHLIGHTS: Summarizing Agent Behavior to People. In *Proceedings of the 17th International Conference on Autonomous Agents and Multi-Agent Systems*, 1168–1176. URL http://dl.acm.org/citation.cfm?id=3237869.
- Ancona, M.; Ceolini, E.; Öztireli, C.; and Gross, M. 2018. Towards better understanding of gradient-based attribution methods for Deep Neural Networks. In *6th International Conference on Learning Representations*. URL https://openreview.net/forum?id=Sy21R9JAW.
- Anderson, A.; Dodge, J.; Sadarangani, A.; Juozapaitis, Z.; Newman, E.; Irvine, J.; Chattopadhyay, S.; Fern, A.; and Burnett, M. 2019. Explaining Reinforcement Learning to Mere Mortals: An Empirical Study. In *Proceedings of the Twenty-Eighth International Joint Conference on Artificial Intelligence, IJCAI-19*, 1328–1334. International Joint Conferences on Artificial Intelligence Organization. URL https://doi.org/10.24963/ijcai.2019/184.
- Arrieta, A. B.; Rodríguez, N. D.; Ser, J. D.; Bennetot, A.; Tabik, S.; Barbado, A.; García, S.; Gil-Lopez, S.; Molina, D.; Benjamins, R.; Chatila, R.; and Herrera, F. 2020. Explainable Artificial Intelligence (XAI): Concepts, taxonomies, opportunities and challenges toward responsible AI. *Inf. Fusion* 58: 82–115. doi:10.1016/j.inffus.2019. 12.012.
- Bach, S.; Binder, A.; Montavon, G.; Klauschen, F.; Müller, K.-R.; and Samek, W. 2015. On pixel-wise explanations for non-linear classifier decisions by layer-wise relevance propagation. *PloS one* 10(7).
- Bellemare, M. G.; Naddaf, Y.; Veness, J.; and Bowling, M. 2013. The Arcade Learning Environment: An Evaluation Platform for General Agents. *J. Artif. Intell. Res.* 47: 253–279. doi:10.1613/jair.3912. URL https://doi.org/10.1613/jair.3912.
- Dhariwal, P.; Hesse, C.; Klimov, O.; Nichol, A.; Plappert, M.; Radford, A.; Schulman, J.; Sidor, S.; Wu, Y.; and Zhokhov, P. 2017. OpenAI Baselines. https://github.com/openai/baselines.
- Greydanus, S.; Koul, A.; Dodge, J.; and Fern, A. 2018. Visualizing and Understanding Atari Agents. In *Proceedings of the 35th International Conference on Machine Learning*, 1787–1796. URL http://proceedings.mlr.press/v80/greydanus18a.html.
- Huber, T.; Weitz, K.; André, E.; and Amir, O. 2020. Local and Global Explanations of Agent Behavior: Integrating Strategy Summaries with Saliency Maps. *CoRR* abs/2005.08874. URL https://arxiv.org/abs/2005.08874.
- Kindermans, P.; Schütt, K. T.; Alber, M.; Müller, K.; Erhan, D.; Kim, B.; and Dähne, S. 2018. Learning how to explain neural networks: PatternNet and PatternAttribution.

- In 6th International Conference on Learning Representations. OpenReview.net. URL https://openreview.net/forum?id=Hkn7CBaTW.
- Mnih, V.; Kavukcuoglu, K.; Silver, D.; Rusu, A. A.; Veness, J.; Bellemare, M. G.; Graves, A.; Riedmiller, M.; Fidjeland, A. K.; Ostrovski, G.; et al. 2015. Human-level control through deep reinforcement learning. *nature* 518(7540): 529–533.
- Mohseni, S.; Zarei, N.; and Ragan, E. D. 2020. A Multidisciplinary Survey and Framework for Design and Evaluation of Explainable AI Systems.
- Mollahosseini, A.; Hasani, B.; and Mahoor, M. H. 2017. Affectnet: A database for facial expression, valence, and arousal computing in the wild. *IEEE Transactions on Affective Computing* 10(1): 18–31.
- Parkhi, O. M.; Vedaldi, A.; and Zisserman, A. 2015. Deep Face Recognition. In Xie, X.; Jones, M. W.; and Tam, G. K. L., eds., *Proceedings of the British Machine Vision Conference 2015*, 41.1–41.12. BMVA Press. URL https://doi.org/10.5244/C.29.41.
- Petsiuk, V.; Das, A.; and Saenko, K. 2018. Rise: Randomized input sampling for explanation of black-box models. *arXiv preprint arXiv:1806.07421*.
- Ribeiro, M. T.; Singh, S.; and Guestrin, C. 2016. "Why should i trust you?" Explaining the predictions of any classifier. In *Proceedings of the 22nd ACM SIGKDD international conference on knowledge discovery and data mining*, 1135–1144.
- Samek, W.; Binder, A.; Montavon, G.; Lapuschkin, S.; and Müller, K. 2017. Evaluating the Visualization of What a Deep Neural Network Has Learned. *IEEE Trans. Neural Networks Learn. Syst.* 28(11): 2660–2673. URL https://doi.org/10.1109/TNNLS.2016.2599820.
- Schulz, K.; Sixt, L.; Tombari, F.; and Landgraf, T. 2020. Restricting the Flow: Information Bottlenecks for Attribution. In 8th International Conference on Learning Representations. URL https://openreview.net/forum?id=S1xWh1rYwB.
- Selbst, A. D.; and Barocas, S. 2018. The intuitive appeal of explainable machines. *Fordham L. Rev.* 87: 1085.
- Selvaraju, R. R.; Cogswell, M.; Das, A.; Vedantam, R.; Parikh, D.; and Batra, D. 2020. Grad-CAM: Visual Explanations from Deep Networks via Gradient-Based Localization. *Int. J. Comput. Vis.* 128(2): 336–359. URL https://doi.org/10.1007/s11263-019-01228-7.
- Simonyan, K.; Vedaldi, A.; and Zisserman, A. 2014. Deep Inside Convolutional Networks: Visualising Image Classification Models and Saliency Maps. In *2nd International Conference on Learning Representations*. URL http://arxiv.org/abs/1312.6034.
- Sixt, L.; Granz, M.; and Landgraf, T. 2019. When Explanations Lie: Why Modified BP Attribution Fails. *CoRR* abs/1912.09818. URL http://arxiv.org/abs/1912.09818.
- Stone, P.; Brooks, R.; Brynjolfsson, E.; Calo, R.; Etzioni, O.; Hager, G.; Hirschberg, J.; Kalyanakrishnan, S.; Kamar, E.;

Kraus, S.; Leyton-Brown, K.; Parkes, D.; William, P.; AnnaLee, S.; Julie, S.; Milind, T.; and Astro, T. 2016. Artificial intelligence and life in 2030. *One Hundred Year Study on Artificial Intelligence: Report of the 2015-2016 Study Panel*

.

Sundararajan, M.; Taly, A.; and Yan, Q. 2017. Axiomatic Attribution for Deep Networks. In Precup, D.; and Teh, Y. W., eds., *Proceedings of the 34th International Conference on Machine Learning*, volume 70 of *Proceedings of Machine Learning Research*, 3319–3328. PMLR. URL http://proceedings.mlr.press/v70/sundararajan17a.html.

tf explain. 2019. Interpretability methods for tf.keras models with Tensorflow 2.0. https://github.com/sicara/tf-explain.

Zeiler, M. D.; and Fergus, R. 2014. Visualizing and understanding convolutional networks. In *European conference on computer vision*, 818–833. Springer.